

# Dielectric Relaxation Formation by Hen Egg White Lysozyme

Dr. Yathrib Ajaj, PhD

College of Science, Mathematics and Sciences Department  
German University of Technology in Oman-Oman

**Abstract:-** Conformational changes of proteins can be resolved by DRS. In the DRS measurement, an alternating voltage is applied across a sample and the sinusoidal current as a response is obtained as a function of frequency. On the basis of the measurement result, the complex permittivity and conductance can be calculated. The complex permittivity can be related with properties determined by the charge response in a system. However, the dielectric properties at low frequency (smaller than 100 MHz) is related with the overall effective dipole moment change of molecules, because the results at low frequencies are primarily determined by the polarization of the whole protein and can indicate the overall structural change (i.e., the progress of the fibrillization). Moreover, as proteins are aggregated and form bigger oligomers or plaques, the dielectric relaxation spectroscopy and the hydrodynamical change can generate an additional characterization data of protein fibrillization.

**Keywords:-** Dielectric Relaxation, Lysozyme, Permittivity, Hydrodynamic Radius, Dipole Moment, Aggregation, Amyloid, Folding.

## I. INTRODUCTION

A wide range of proteins is known to misfold and aggregate in mildly denaturing conditions into large polymeric structures known as amyloid fibrils. These fibrils are found to be associated with a variety of disorders including Alzheimer's disease, Parkinson's disease, Huntington's disease, prion diseases and type II diabetes<sup>1-3</sup>. The fibrils can also be formed in vitro, from proteins associated with a disease, as well as proteins associated with none<sup>4</sup>.

Amyloid fibrils share some common features, consisting of continuous intermolecular  $\beta$ -sheets which run along the fibril axis, such that the individual  $\beta$ -strands are perpendicular to the fibril axis<sup>5</sup>. This common structural motif based only on the peptide backbone, as well as the observation that a wide variety of proteins forms these fibrils, suggests that amyloid fibrils are a generic form of protein assembly structure<sup>6</sup>. Electron microscopy revealed that amyloid fibrils are straight, unbranching fibrils with diameters around 10 nm<sup>7</sup>.



Fig 1

Hen egg white lysozyme (LYS) has been found to form amyloid fibrils in vitro<sup>8, 9</sup>. LYS is a very well characterized bacteriolytic enzyme, synthesized by macrophages in the liver<sup>10, 11</sup> and is also present at high concentrations cartilage, milk, and saliva. It is also one of the best characterized and most studied of all proteins. Furthermore, LYS is homologous to human LYS, which is involved in amyloid-related human disorders<sup>12</sup> and for which aggregation is also observed in vitro<sup>13</sup>. In all the reported cases, the disease is associated with single point mutations in the LYS gene and fibrils appear to be deposited widely in tissue<sup>12</sup>. Subsequently, it was shown that LYS could form fibrils in vitro. Work from Dobson's group revealed that lowering the pH to 2.0 and raising the temperature to 57 °C result in amyloid fibrils<sup>13</sup>. The formation of amyloid aggregates in vitro by wild-type and point mutated human LYS has been studied by Morozova-Roche *et al.*<sup>13</sup>. Amyloid fibril formation was observed upon incubation of the wild-type and the variant human LYSs at conditions where partially folded intermediates are highly populated. Seeding experiments proved that the fibril formation was greatly influenced by the presence of the seeds.

Conformational changes of proteins can be resolved by DRS. In the DRS measurement, an alternating voltage is applied across a sample and the sinusoidal current as a response is obtained as a function of frequency. Based on the measurement result, the complex permittivity and conductance can be calculated. The complex permittivity can be related with properties determined by the charge response in a system. However, the dielectric properties at low frequency (smaller than 100 MHz) is related with the overall effective dipole moment change of molecules,

because the results at low frequencies are primarily determined by the polarization of the whole protein and can indicate the overall structural change (i.e., the progress of the fibrillization). Moreover, as proteins are aggregated and form bigger oligomers or plaques, the dielectric relaxation spectroscopy and the hydrodynamical change can generate an additional characterization data of protein fibrillization.

## II. MATERIAL AND INSTRUMENTATION

### ➤ Materials

Hen egg white lysozyme, LYS, ( $\geq 90\%$ , L 7651) was purchased from Sigma-Aldrich as dialyzed and lyophilized powder and used without further purification. Stock solution of LYS was prepared by solubilisation of protein powders in 30 mM acetate buffer (pH 4). It was filtered through a 0.2  $\mu\text{m}$  membrane. The protein concentrations were determined by measuring the absorbance at 280 nm using extinction coefficients of 38782 L mol<sup>-1</sup> cm<sup>-1</sup> for LYS. The solutions were incubated at 70 °C up to 6 days.

### ➤ Dielectric Relaxation Spectroscopy

Since the aim was to uncover the protein relaxation ( $\beta$ -relaxation) mechanism, the frequency coverage was restricted to values between 1 MHz  $< \nu < 1300$  MHz. The experimental uncertainty was within the range 1-5 % at all the frequencies.

The effective hydrodynamic radius and the electrical dipole moment are calculated to further characterize the oligomerization and aggregation of protein based on the DRS result. First, the Debye equation as a dielectric relaxation model is applied to obtain the relaxation time and amplitude:

$$\varepsilon^*(\nu) = \varepsilon_\infty + \frac{\Delta\varepsilon}{1 + i(2\pi\nu\tau)^2} \quad 1$$

where  $\varepsilon^*(\nu) = \varepsilon'(\nu) - i\varepsilon''(\nu)$  is the complex permittivity,  $\nu$  is the frequency,  $\tau$  is the relaxation time  $\Delta\varepsilon = \varepsilon_0 - \varepsilon_\infty$  is the increment of the dielectric constant,  $\varepsilon_0$  and  $\varepsilon_\infty$  are the dielectric constant at low and infinite frequency, respectively. As usual, the imaginary part,  $\varepsilon''$ , i.e. the dielectric loss, exhibited a contribution due to the d.c. conductivity,  $\sigma$ , of the form:

$$\varepsilon''(\nu) = \frac{\sigma}{2\pi\varepsilon_0\nu} \quad 2$$

A superposition of two exponential processes yields a Lorentzian shape of  $\varepsilon'(\nu)$  and  $\varepsilon''(\nu)$  according to:

$$\varepsilon'(\nu) = \varepsilon_\infty + \sum_{j=1}^2 \frac{S_j}{1 + (2\pi\nu\tau_j)^2} \quad 3$$

$$\varepsilon''(\nu) = \sum_{j=1}^2 \frac{2\pi\nu S_j}{1 + (2\pi\nu\tau_j)^2} \quad 4$$

### ➤ Differential Scanning Calorimetry (DSC)

Differential scanning calorimetry (DSC) was carried out using a MicroCal VP-DSC differential scanning microcalorimeter (MicroCal LLC, GE Healthcare, Northampton, MA). Evaluation of the thermodynamic data was done with the manufacturer's software (Microcal Origin 4.1).

## III. RESULTS AND DISCUSSION

The effect of temperature on fibril formation from hen egg white lysozyme (LYS) was studied using DRS. Fibril formation is promoted by low pH and temperatures close to the midpoint temperature for protein unfolding. Nucleation presumably involves a change in the conformation of individual LYS molecules.

Figure 1 shows the tumbling time dependence of the LYS solution at pH 4.0 in 10 mM acetate buffer as the incubation time was varied from 0 to 7 days. The increase of incubation time is accompanied by an increase in relaxation time, which means that the LYS tumbling becomes slower. The abrupt increase of the relaxation time may result from the formation of amyloid fibril.

Moreover, the effective hydrodynamic radius is calculated to further characterize the oligomerization and aggregation of LYS based on the DRS result. First, the 2D Debye equation as a dielectric relaxation model is applied to obtain the relaxation frequency. From this relaxation frequency, the effective hydrodynamic radius,  $r_h$ , which represents the status of the fibrillized LYS, can be calculated using Equation 5, under the assumption that the shape of LYS is spherical. Table 1 shows the determined hydrodynamic radius as a function of incubation time. It indicates a systematic increase from 2.13 to 3.40 nm with increasing incubation time.

$$r_h = \sqrt[3]{\frac{k_B T}{4\pi\eta} \tau_\beta} \quad 5$$

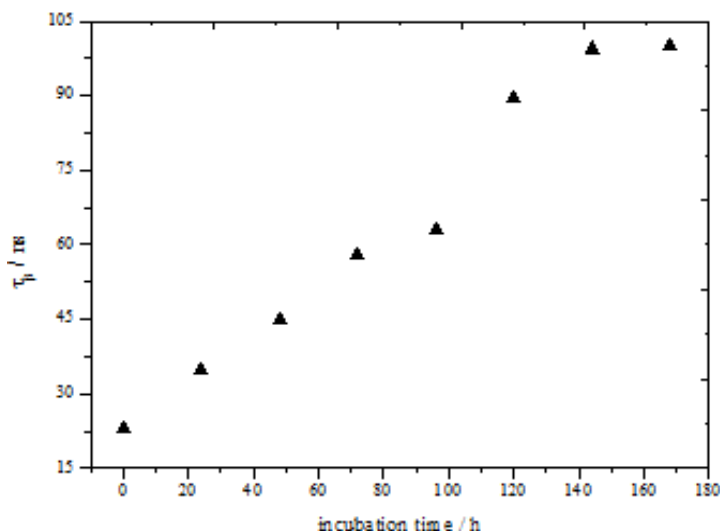


Fig 2:- Relaxation time of 1.7 mM HEWL incubated at 70 °C and pH 4.

The variation of the dielectric increment relaxation amplitude of LYS as a function of incubation time is illustrated in Figure 2. The amplitude of the  $\beta$ -relaxation increased as the incubation time increased. In fact, the amplitude is linearly dependent on incubation time.

The relaxation amplitudes were used to estimate the dipole moment of LYS as a function of incubation time. Recalling the most frequently employed Onsager-Onccley equation, we have:

$$\mu_{eff} = \sqrt{\frac{2\epsilon_0 k_B T}{N_A c_p}} S_{\beta} \tag{6}$$

The dipole moment enables one to understand electrostatic effects. Assuming that the overall effective dipole moment of the aggregated LYS is relatively small compared with soluble LYS monomer due to the size, this change in dipole moment during the fibrilization can induce longer momentary delay with respect to the alternating electrical field. Thus, the intensity growth in permittivity is observed.

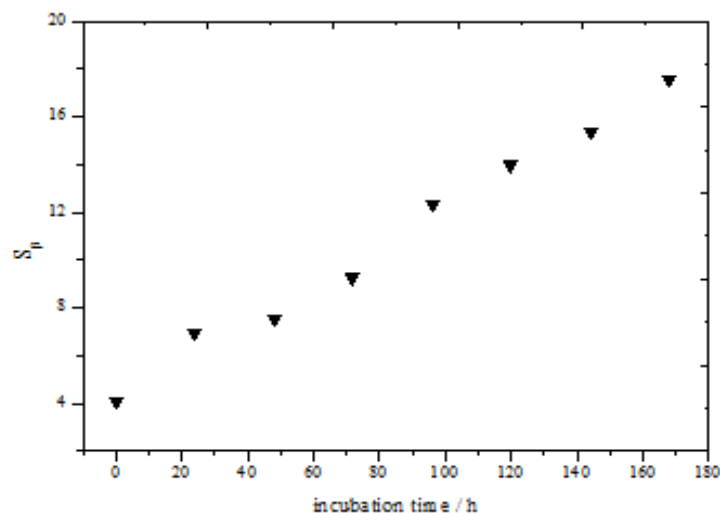


Fig 3:- Relaxation amplitude of 1.7 mM LYS incubated at 70 °C and pH 4.

Overall, the amyloid fibril assembly of LYS followed a strict hierarchical aggregation pathway, with amyloid monomers, oligomers, and protofibrils forming on-pathway intermediates for assembly into successively more complex structures. For such system, the polarization is controlled by the average dipole moment. The observed  $\mu_{eff}$  values are expected to reflect an average dipole moment between the purely monomeric LYS and higher order aggregates.

The two populations cannot be resolved by DRS. Hence, no specific information was provided about the morphology of any of the intermediate aggregate species. To address these shortcomings, differential scanning calorimetry (DSC) on LYS undergoing fibril formation was performed.

To correlate DSC data with DRS measurements, LYS fibrillogenesis was monitored using DRS while small aliquots were withdrawn for DSC scans at various times during the incubation period. The slope from the linear fit of  $\Delta H_{integ}$  against melting temperature  $T_m$  gives an estimate of  $C_p$ . Figure 3 shows that  $C_p$  is dependent on

incubation time within the condition of this experiment. The concentration of folded soluble LYS was calculated by the area under the unfolding peak. As it appears from the Figure, the area under the unfolding peak decreases monotonously upon incubation. The results of this experiment are summarized in Table 1.

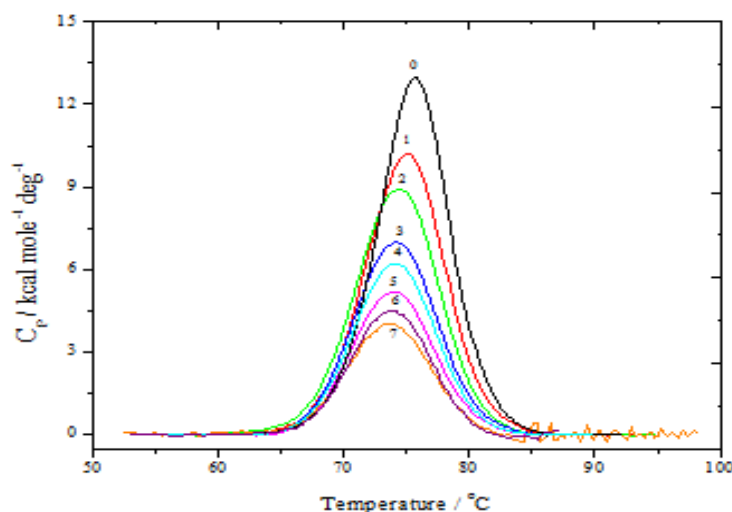


Fig 4:- DSC thermograms of amyloid fibrils of HEWL and pH 4. Fibril samples incubated at 70 °C. The numbers represent the incubation days.

Incubation days	Folded LYS concentration mM	$r_{hd} / nm$	$\mu_{eff} / D$ (monomer)	$\mu_{eff} / D$ (oligomers)
0	1.70	2.13	145	0
1	1.69	2.34	158	1550
2	1.59	2.54	164	524
3	1.07	2.75	183	279
4	0.98	2.82	204	337
5	0.92	3.20	224	358
6	0.73	3.32	235	345
7	0.68	3.40	277	349

Table 1:- The concentration of LYS and physical parameters (1.7 mM, pH 4) incubated at 70°C.

From Table 1 for folded LYS the effective dipole moment increases with increase in incubation time, whereas the dipole moment of oligomers decreases. As noted, many previous studies imply that LYS form aggregates upon incubation at 70 °C. Our observation confirms this view. The concentration dependence of the effective dipole moments contains information about mutual correlations among the dipoles<sup>15</sup>. The relation 5 was derived by the assumption that there is no inter-correlation among the dipoles of the protein. But, the variation of dipole moment here convincingly demonstrates that there is a strong correlation.

#### IV. CONCLUSION

Here, the benefits of DRS in enhancing the knowledge of protein self-association in solutions were illustrated. The current study demonstrates a competitive assembly of proteins fibrils by varying incubation time. Dielectric relaxation spectroscopy in the megahertz to gigahertz regime was used to study the aggregation hen egg white lysozyme, LYS. Dielectric spectra in the megahertz to gigahertz regime were recorded for several samples with different incubation time over a period up to seven days at time intervals of 24 hours. The dielectric spectra data allow to deconvolute a relaxation regime due to the tumbling motion of the protein and its aggregates. The evaluation of the dielectric relaxation data allowed to follow the evolution of the tumbling times and hydrodynamic radii due to protein aggregation. The fibril’s hydrodynamic radii and dipole moments increase with increasing the incubation

time. To confirm the formation of higher oligomers, differential scanning calorimetry (DSC) on LYS undergoing fibril formation was performed. DSC data show that the concentration of the native LYS monomer decreases monotonously upon incubation.

### REFERENCES

- [1]. Stenstad, T.; Magnus, J. H. and Husby, G. *The Biochem. J.*, **1994**, 303, 663-70.
- [2]. Kelly, J.W. *Curr. Opin. Struct. Biol.*, **1996**, 6, 11.
- [3]. Sunde, M.; Serpell L. C.; Bartlam, M.; Fraser, P. E.; Pepys, M. B. and Blake, C. C. *J Mol Biol.*, **1997**, 273.
- [4]. Lashuel, H. A.; LaBrenz, S. R.; Woo, L.; Serpell, L.C. and Kelly, J. W. *J. Am. Chem. Soc.*, **2000**, 122, 5262.
- [5]. Dobson, M. *Trends Biochem. Sci.*, **1999**, 24, 329.
- [6]. Shirahama, T. and Cohen, A. S. *J. Cell Biol.*, **1967**, 33, 679.
- [7]. Goda, S.; Takano, K.; Yamagata, Y.; Nagata, R.; Akutsu, H.; Maki, S.; Namba, K. and Yutani, K. *Protein Sci.*, **2000**, 9, 369.
- [8]. Krebs, M. R.; Wilkins, D. K.; Chung, E. W.; Pitkeathly, M. C.; Chamberlain, A. K.; Zurdo, J.; Robinson, C. V. and Dobson, C. M. *J. Mol. Biol.*, **2000**, 300, 541.
- [9]. Melrose, J.; Ghosh, P. and Taylor, T. K. F. *Gerontology*, **1989**, 35, 173.
- [10]. Porstmann, B.; Juns, K.; Schmechta, H.; Evers, U.; Persande, M.; Porstmann, T.; Kram, J. and Krause, H. *Clin. Biochem.*, **1989**, 22, 349.
- [11]. Pepys, M. B.; Hawkins, P. N.; Booth, D. R.; Vigushin, D. M.; Tennent, G. A.; Soutar, A. K.; Totty, N., Nguyen, O.; Blake, C. C. F.; Terry, C. J.; Feest, T. G.; Zalin, A. M. and Hsuan, J. J. *Nature*, **1993**, 362, 553.
- [12]. Morozova-Roche, L. A. J.; Zurdo, J.; Spencer, A.; Noppe, W.; Pepys, M.; Receveur, V. and Dobson, C. M. *J. Struct. Biol.*, **2000**, 130, 339.
- [13]. Nettleton, E. J.; Tito, P.; Sunde, M.; Bouchard, M.; Dobson, C. M. and Robinson, C. V. *Biophys. J.*, **2000**, 79, 1053.
- [14]. Ajaj, Y.; Wehner, M. and Weingärtner, H. *Zeitschrift für Physikalische Chemie.*, **2009**, 223, 1105.